







Vasopressin acts as a synapse organizer in limbic regions by boosting PSD95 and GluA1 expression

Limei Zhang¹  | Teresa Padilla-Flores¹ | Vito S. Hernández¹  |
 Mario A. Zetter¹  | Elba Campos-Lira¹ | Laura I. Escobar¹  |
 Robert P. Millar^{1,2,3}  | Lee E. Eiden⁴ 

¹Department of Physiology, School of Medicine, National Autonomous University of Mexico, Mexico City, Mexico

²Centre for Neuroendocrinology, Department of Immunology, University of Pretoria, Pretoria, South Africa

³Department of Integrative Biomedical Sciences, Institute of Infectious Disease and Molecular Medicine, University of Cape Town, Cape Town, South Africa

⁴Section on Molecular Neuroscience, NIMH-IRP, NIH, Bethesda, Maryland, USA

Correspondence

Limei Zhang, Department of Physiology, School of Medicine, National Autonomous University of Mexico, Av. Universidad 3000, CDMX, 04510, Mexico.
 Email: limei@unam.mx

Lee E. Eiden, Section on Molecular Neuroscience, NIMH-IRP, NIH, Bethesda, MD, USA.
 Email: eidenl@nih.gov

Funding information

Consejo Nacional de Ciencia y Tecnología, México CONACYT, Grant/Award Numbers: A1-S8731, CB-283279, CONACYT-CB-238744; National Institute of Mental Health, Grant/Award Number: ZIAMH0002386; Universidad Nacional Autónoma de México, Grant/Award Number: GI200121; CONACYT

Abstract

Hypothalamic arginine vasopressin (AVP)-containing magnocellular neurosecretory neurons (AVPMNN) emit collaterals to synaptically innervate limbic regions influencing learning, motivational behaviour, and fear responses. Here, we characterize the dynamics of expression changes of two key determinants for synaptic strength, the postsynaptic density (PSD) proteins AMPAR subunit GluA1 and PSD scaffolding protein 95 (PSD95), in response to *in vivo* manipulations of AVPMNN neuronal activation state, or exposure to exogenous AVP *ex vivo*. Both long-term water deprivation *in vivo*, which powerfully upregulates AVPMNN metabolic activity, and exogenous AVP application *ex vivo*, in brain slices, significantly increased GluA1 and PSD95 expression as measured by western blotting, in brain regions reportedly receiving direct ascending innervations from AVPMNN (i.e., ventral hippocampus, amygdala and lateral habenula). By contrast, the visual cortex, a region not observed to receive AVPMNN projections, showed no such changes. *Ex vivo* application of V1a and V1b antagonists to ventral hippocampal slices ablated the AVP stimulated increase in postsynaptic protein expression measured by western blotting. Using a modified expansion microscopy technique, we were able to quantitatively assess the significant augmentation of PSD95 and GLUA1 densities in subcellular compartments in locus coeruleus tyrosine hydroxylase immunopositive fibres, adjacent to AVP axon terminals. Our data strongly suggest that the AVPMNN ascending system plays a role in the regulation of the excitability of targeted neuronal circuits through upregulation of key postsynaptic density proteins corresponding to excitatory synapses.

KEYWORDS

central amygdala, expansion microscopy, ventral hippocampus, water deprivation, western blotting

Limei Zhang, Teresa Padilla-Flores, Vito S. Hernández, and Mario A. Zetter contributed equally to this work.

This is an open access article under the terms of the [Creative Commons Attribution-NonCommercial-NoDerivs](https://creativecommons.org/licenses/by-nc-nd/4.0/) License, which permits use and distribution in any medium, provided the original work is properly cited, the use is non-commercial and no modifications or adaptations are made.

© 2022 The Authors. *Journal of Neuroendocrinology* published by John Wiley & Sons Ltd on behalf of British Society for Neuroendocrinology.

1 | INTRODUCTION

The neurohormone arginine vasopressin (AVP, also called antidiuretic hormone) is mainly synthesized in the hypothalamic paraventricular and supraoptic nuclei by a type of cell with large somata (diameters around 20–35 μm) that are traditionally referred to as magnocellular neurosecretory neurons (AVPMNN) and is released mainly in the posterior hypophysis as the key regulator of body water homeostasis.¹ The AVPMNN, together with those for oxytocin, were the first peptidergic systems to be described in the mammalian brain.² Release of AVP from both posterior pituitary lobe and median eminence, as well as AVPMNN somatodendritic release within the hypothalamus itself,^{3,4} helps to control water homeostasis.

In the 1970s, David de Wied pioneered studies suggesting that vasopressin may act as a neurotransmitter or neuromodulator at synapses within the brain cognitive/emotional control centres.^{5,6} Shortly afterward, a series of studies published in the 1980s and early 1990s showed that submicromolar concentrations of vasopressin could, in brain slices *ex vivo*, powerfully and reversibly increase the rate of firing of neurons in the CA1 areas of rat hippocampal slices and that this effect could be fully antagonized by an anti-vasopressor vasopressin analogue.⁷ Subsequently, AVP was localized to Gray type I synapses, usually corresponding to glutamatergic (excitatory) neurotransmission,⁸ in hippocampus,⁹ amygdala,¹⁰ lateral habenula,¹¹ and locus coeruleus (LC).¹² These observations cemented the notion that AVP could act within the brain as well as in the periphery through AVP release from the same neurons, which therefore integrated regulation of homeostatic (hydromineral balance) and allostatic (behavioural) physiology within a single type of neurohormonal/neuropeptide cell.^{13,14}

Despite the plethora of observations detailing AVP actions at hippocampal and other cognitive hubs in the brain (*vide supra*), the cellular mechanisms by which AVP potentiates neuronal excitability are not known. AVP-containing dense core vesicles (AVP+ DCV) have been observed at excitatory synaptic active zones, docked onto the presynaptic membrane, suggesting that vasopressin modulation of neurotransmission may occur at the level of the synapse itself within limbic regions such as hippocampus,⁹ amygdala,¹⁰ lateral habenula,¹¹ and LC.¹² Figure 1 summarizes previous works showing this phenomenon in lateral habenula, A, and ventral hippocampus, B, as two examples. In both cases, the animals were under food and water *ad libitum* intake conditions before fixation.

With this background, we considered whether AVP could participate in the modulation of synapse strength via dynamic modification of the protein composition of the postsynaptic density (PSD). We characterized the dynamic expression changes of two PSD proteins, AMPAR subunit GluA1 and PSD scaffolding protein 95 (PSD95), which are known to be key determinants for synaptic strength, under *in vivo* and *ex vivo* conditions. Both long-term water deprivation (WD) *in vivo*, which powerfully upregulates AVPMNN metabolic activity, and exogenous AVP application, in *ex vivo* brain slices, significantly increased GluA1 and PSD95 expressions as measured by western blotting, in brain regions that receive direct ascending innervations from AVPMNN (*i.e.*, ventral hippocampus, amygdala, and lateral habenula, *vide supra*), whereas the visual cortex, a region not observed to receive AVPMNN projections, showed no significant differences. *Ex vivo* application of V1a and V1b antagonists to ventral hippocampal slices ablated the AVP stimulated increase in postsynaptic protein expression measure by western blotting.

Efforts to localize the PSD95 and GluA1 immunopositive puncta in the postsynaptic segment, in an identified cell type, adjacent to

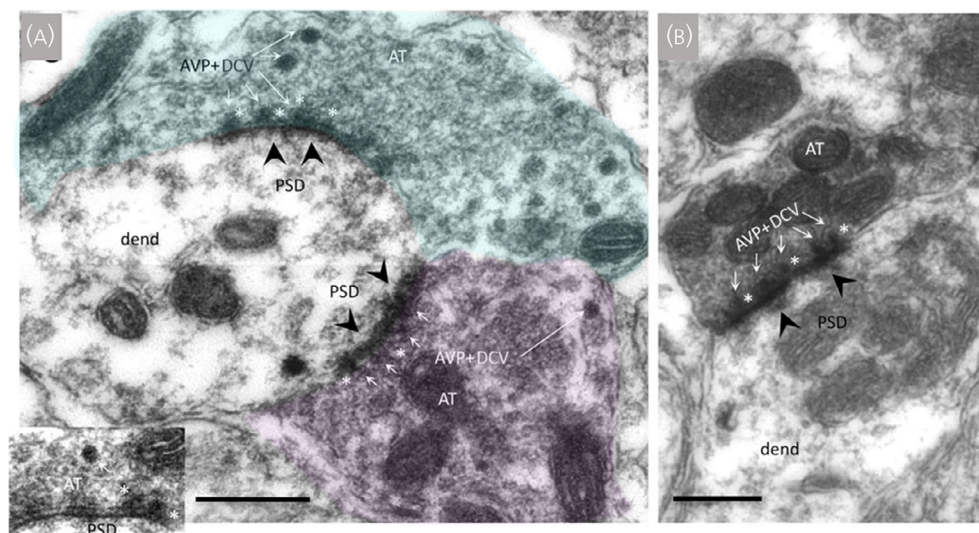


FIGURE 1 Ultrastructural examples showing morphological evidence that arginine vasopressin (AVP) could directly modulate synaptic function. (A) two Gray type I synapses made by two AVP-immunopositive (AVP+) axon terminals (AT, green and pink) onto an unlabeled dendrite (dend) contain AVP-containing dense core vesicles (AVP+ DCV) (white arrows). Inset: higher magnification of four AVP+ DCV docked on the active zone of the presynaptic membrane. Postsynaptic density (PSD), a morphological feature of glutamatergic synapse, is indicated by a black arrowhead. Sample was taken from rat lateral habenula. (B) Analogue notations to (A), with a sample taken from rat ventral hippocampus. In both cases, the animals were under food and water *ad libitum* intake conditions before fixation. (A) Modified from Zhang et al.¹¹ (Creative Commons Attribution License holder). (B) Reproduced with permission from Zhang and Hernandez.⁹ Scale bars: 500 nm

AVP immunopeptide axons, were further made. Because of the tight association of the axonal bouton and the dendritic spine, which limits the clear distinction under conventional confocal microscopy, we took advantage of newly developed expansion microscopy (ExM) technique,^{15–17} which utilizes isotropic tissue swelling to expand the sample, so that the resolving power to visualize the PSD proteins under regular confocal imaging can achieve the necessary resolution required to quantitatively assess the PSD95 and GluA1 immunopositive puncta densities. We observed significant augmentation of PSD95 and GLUA1 densities in the LC, a region demonstrated to receive direct AVPMNN innervation,¹² under WD conditions, within an identified cell type (TH+ neurons) adjacent to AVP axon terminals.

2 | MATERIALS AND METHODS

2.1 | Rats

In total, 56 male Wistar rats weighing 250 ± 50 g were used in the present study. Rats were obtained from the local animal vivarium and were housed three per cage under controlled temperature and illumination (12:12 h light/dark photocycle) with water and chow ad libitum unless otherwise indicated. All animal procedures were approved by the local research ethics supervision commission (license number CIEFM-079-2020).

2.2 | Chemical and primary antibodies

Arginine vasopressin (MK I-23) for western blotting experiment was kindly donated by Professor Maurice Manning.¹⁸ AVP receptor antagonists, V1b (SSR149415) and V1a (SR49059), were provided by Axon Medchem (Groningen, The Netherlands). Primary antibodies used for western blotting experiments were: mouse monoclonal anti-PSD95 (clone K28/74; 1 mg mL^{-1} , dilution 1:1000; UC Davis, Davis, CA, USA), guinea pig polyclonal anti-GluR1 (GluA1-GP-Af380; $200 \mu\text{g mL}^{-1}$, dilution 1:1000; Frontiers Sendai, Institute, Japan; <https://nittobo-nmd.co.jp/pdf/reagents/GluA1.pdf>), and mouse monoclonal anti-GAPDH (GTX627408; dilution 1:2000; GeneTex, Irvine, CA, USA); for immunohistochemistry: mouse monoclonal anti-PSD95 (clone K28/74; 1 mg mL^{-1} , dilution 1:1000; UC Davis), guinea pig polyclonal anti-GluR1 (GluA1-GP-Af380; $200 \mu\text{g mL}^{-1}$, dilution 1:1000; Frontiers Institute), sheep anti-tyrosine hydroxylase (TH) (AB1542; Chemicon/Sigma, St Louis, MO, USA), rabbit anti-AVP.¹⁹

The chemicals used for western blotting (standard method) and for expansion microscopy (modified method) are listed in the appropriate sections below.

2.3 | Experimental design

Three sets of experiments (noted as A, B, and C) were performed for the present study.

Experiment A used western blotting method to evaluate changes in PSD95 and GluA1 protein expression levels in an in vivo WD treatment model, in which the variables were different time-points of the treatment. With this physiological treatment, the hypothalamic vasopressin system is known to be upregulated in a relatively selective manner, even before a significant disruption of the body's water homeostasis occurs.²⁰

Experiment B aimed to evaluate, through western blotting, whether the ex vivo, pharmacological exposure of ventral hippocampal slices to AVP 100 nM ,²¹ over different time courses, exerts similar effects on PSD95 and GLUA1 expression as in the WD study, and whether the exposure of equimolar concentrations of its specific antagonists for V1a and V1b receptors, could ablate the increase in expression induced by AVP.

Experiment C was designed to evaluate, through immunohistochemistry and expansion microscopy, whether WD increases the PSD95 and GluA1 immunopositive puncta densities in a given region innervated by AVPMNN direct projection. We chose the pontine LC as an example of a region densely innervated by AVP-immunopositive fibres that further increases in immunolabeling density with WD.¹² The strong somatic/dendritic expression of TH and the cell population homogeneity of the LC, together with the dense AVP innervation, allowed us to successfully observe the postsynaptic cellular segments contacted by AVP immunopositive fibres, despite the immunofluorescence signals decay with expansion microscopy processing. It is worth noting that the optical resolution of conventional immunofluorescence confocal microscopy limits the quantification of postsynaptic density proteins. With the modified expansion microscopy (2–3 times), this quantification is achievable, at the same time as conserving the regional/cellular structure and ease of specimen handling for microscopical examination.

2.4 | WD treatment and unit-subject definition for western blotting

Twenty-four experimental subjects were divided in four time-points: control (water and food ad libitum), 24 h of WD (24 h WD), 48 h of WD (48 h WD), and 24 h of water restoration after 48 h WD (48 h WD + 24 h R).

To show the dynamic change of PSD95 and GluA1 as a function of the treatment, and to ensure that the samples for each region possessed anatomical precision and sufficient protein amounts, we introduce the unit-subject concept that is defined as protein samples of a given anatomical region coming from eight rats, distributed in four time-points, which were assayed in the same western blotting. The reported results in each time-point have $n = 3$ unit-subjects (six rats in total). The blots of the three unit-subjects, per each region are presented in its entirety in Figure 2, to allow the direct observation of the data, in addition to the numerical data and statistical analysis derived from it (statistic raw data and description are provided in the Supporting information, Appendix S1).

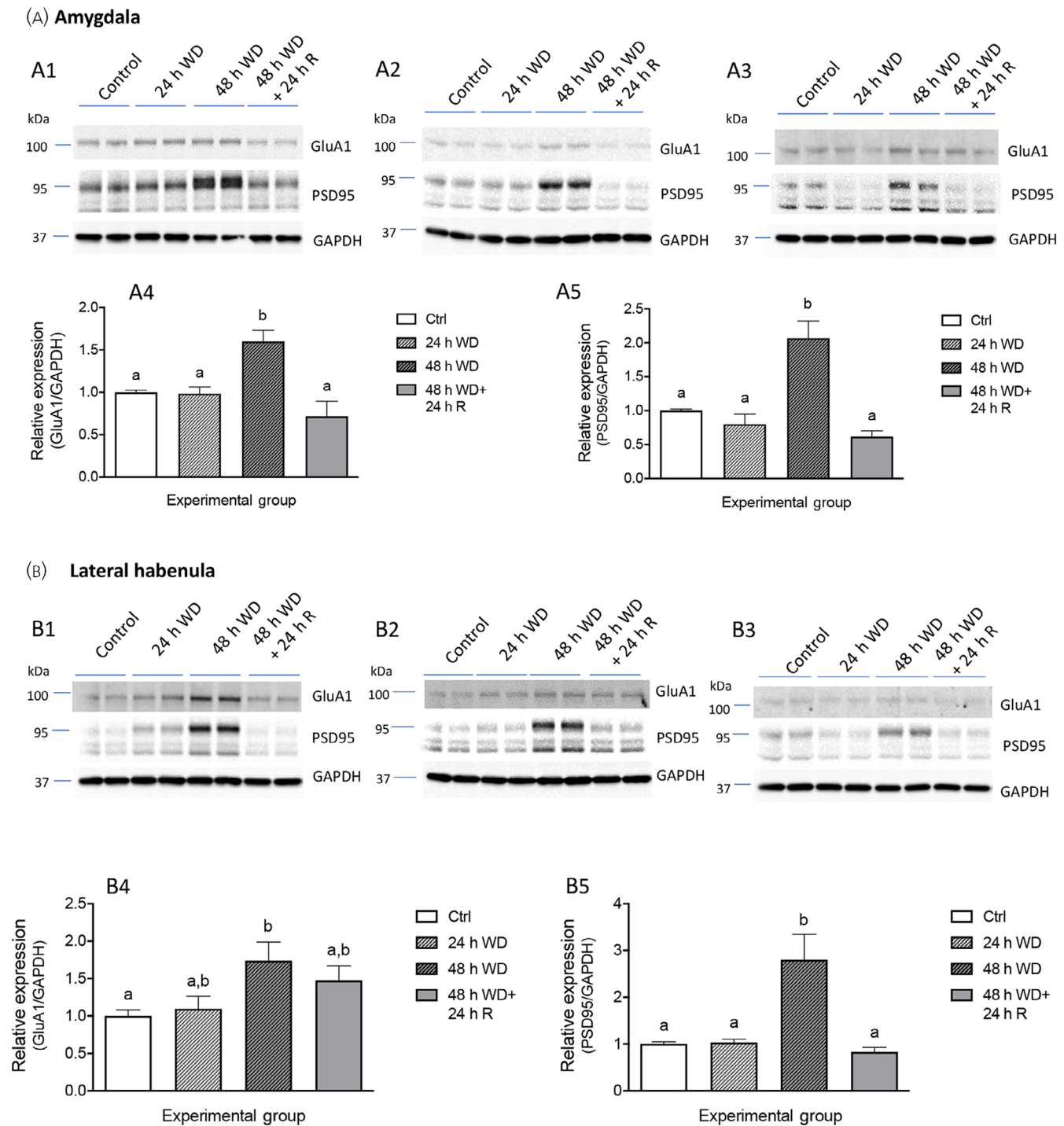


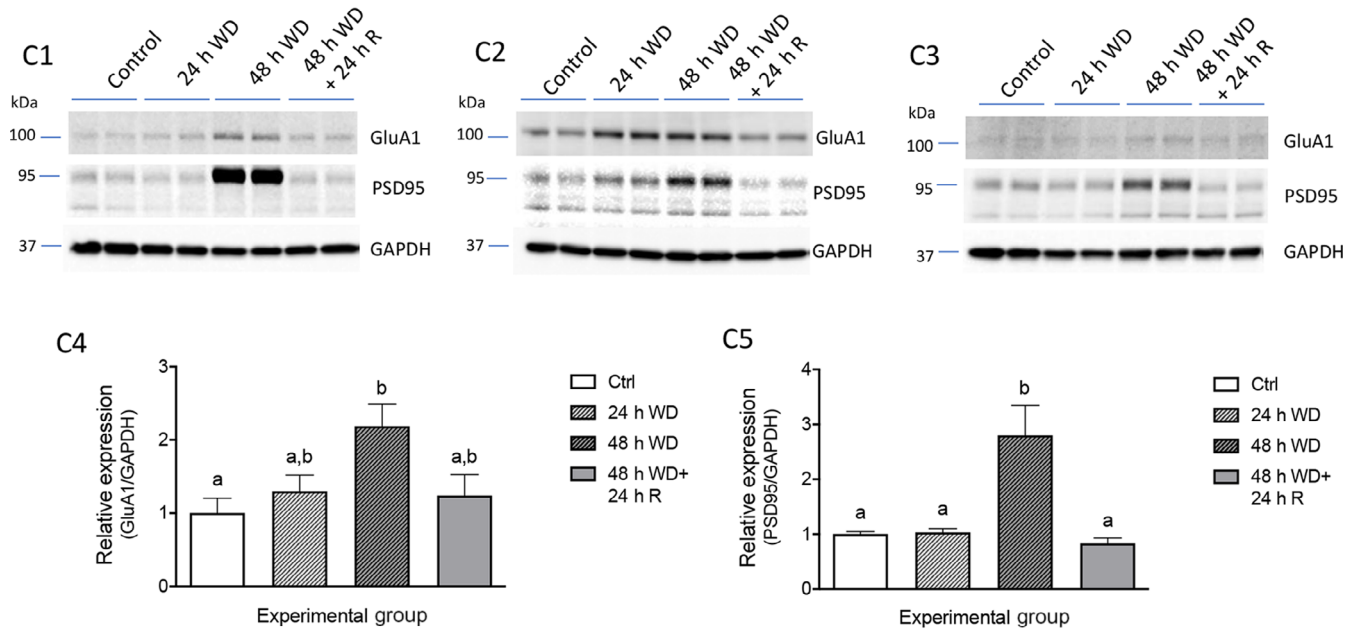
FIGURE 2 Prolonged water deprivation (48 h WD) effectively increased GluA1 and PSD95 expression in the main arginine vasopressin-containing magnocellular neurosecretory neurons (AVPMNN) ascending collaterals targeting regions: amygdala (A), lateral habenula (B); ventral hippocampus (C). We used the primary visual cortex (V1) as a negative control of the experiment (D). The mean relative expression for each treatment was normalized to the expression of the control levels. To show the individual variability and the consistency, as well as the direct basis of the statistic differences, we chose here to show the blots for each of the three unit-subjects; each one includes the complete 4 time-point in duplicates. Bars that do not share a common letter, indicate significant differences between means

2.5 | Sample obtention and western blotting procedure for in vivo experiments

After the corresponding treatment periods (control, 24 h WD, 48 h WD, and 48 h WD + 24 h R), rats were deeply anesthetized with an

overdose of sodium pentobarbital (180 mg kg^{-1} ; Sedalparma, Cancun, México) and decapitated using a rodent guillotine. Fresh brain tissue was removed quickly and dissected on ice-cooled saline (0.9% NaCl) solution. Brains were coronally blocked from optic chiasm (around Bregma 0.00 mm) to posterior Bregma -7.00 mm and put on

(C) Ventral hippocampus



(D) Visual Cortex

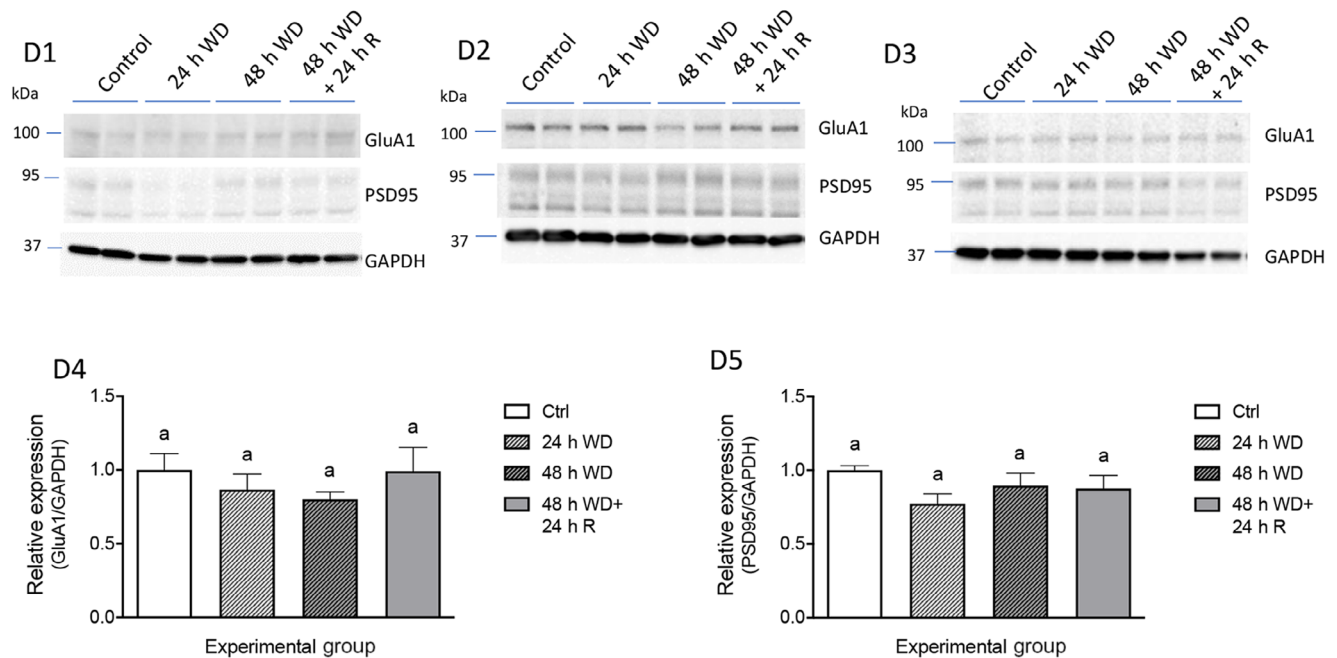


FIGURE 2 (Continued)

a tissue chopper for thick slice preparation (0.5 mm thickness). Segments of brain sections containing central amygdala, habenula, ventral hippocampus (vHi), and primary visual cortex (V1, served as a negative control region because no direct innervations to this region from hypothalamic AVPMNN system have been reported) were obtained under a stereoscopic microscope using microdissection tools. Each sample of a given brain region of interest in this study was pooled

from the same region from two rats to provide sufficient brain tissue for immunoblotting without sacrificing anatomical precision.

Dissected brain regions were sonicated in ice-cold extraction buffer: 50 mM Tris-HCl pH 7.4, 8.5% sucrose, 2 mM ethylenediaminetetraacetic acid, supplemented with proteases and phosphatases inhibitors (8 $\mu\text{g mL}^{-1}$ aprotinin, 10 $\mu\text{g mL}^{-1}$ leupeptin, 4 $\mu\text{g mL}^{-1}$ pepstatin A, 500 μM 4-[2-aminoethyl]benzenesulfonyl fluoride hydrochloride,

5 mM benzamidine, 20 mM β -glycerophosphate, 10 mM sodium fluoride, 1 mM sodium orthovanadate). Brain homogenates were assayed for protein using the BCA method (catalog. no. 23225; Pierce, Thermo Scientific, Waltham, MA, USA). For sodium dodecyl sulfate-polyacrylamide gel electrophoresis (SDS-PAGE), homogenates (15 μ g of total protein) were mixed with loading buffer plus added β -mercaptoethanol and boiled for 3 min. Samples were separated by electrophoresis in 10% acrylamide gels and transferred to 0.2 μ m nitrocellulose membrane (catalog. no. 10600006; GE Healthcare, Chicago, IL, USA). Blots were blocked for 1 h at room temperature in Tris-buffered saline with 0.05% Tween-20 (TBST) containing 5% blotting-grade dry milk (catalog. no. 170-6404; Bio-Rad, Hercules, CA, USA), incubated overnight with primary antibody (dilutions indicated above) in blocking buffer at 4°C, washed 3 \times 10 min in TBST, incubated with secondary antibody conjugated to horseradish peroxidase (dilution 1:5000; Jackson Immuno-Research, West Grove, PA, USA) for 1 h at room temperature, and washed 3 \times 10 min in TBST. Membranes were visualized with luminol substrate by enhanced chemiluminescence.²² PSD95 and GluA1 were evaluated in the same western blots, for which membranes were incubated in stripping buffer (0.2 M glycine pH 2.2, 0.1% SDS, 1% Triton X-100) for 2 \times 15 min at room temperature, washed and re-probed using the above protocol. Antibodies detecting GAPDH or actin were used to provide loading controls.

Blots were scanned with ChemiDoc (Bio-Rad). The images were converted to grayscale and the densitometric analysis was performed using the FIJI Gel analyzer tool (Image J; NIH, Bethesda, MD, USA). Briefly, a rectangular selection was drawn around the bands detecting the postsynaptic proteins GluA1 or PSD-95 and a similar selection around the GAPDH band. In the case of PSD-95, two bands were observed, one at the expected molecular weight of 95 kDa and other around 70 kDa (https://neuromab.ucdavis.edu/datasheet/K28_74.pdf). Because the origin of this lower molecular weight band is controversial, we chose to only measure the band around 95 kDa. After selecting similar size regions, a graph was plotted representing the integrated optical density along the length of the selected area, with the area under the curve representing the optical density of that band. The obtained optical density of PSD95 or GluA1 band was divided over the optical density of the GAPDH band, and the result for each condition was normalized with respect to the average value of the control bands (set to be 1). The results are therefore presented as relative expression of GluA1/loading control or PSD95/loading control.

2.6 | Hippocampal acute slice pharmacology with exogenous AVP

Rats of approximately 200 g were deeply anesthetized using an overdose of sodium pentobarbital (180 mg kg⁻¹; Sedalpharma) and killed by rapid decapitation using a rodent guillotine. Brain horizontal slices of 300 μ m thickness containing the ventral hippocampus were obtained using a VT 1000S vibratome (Leica, Wetzlar, Germany), in ice-cold cutting solution containing (in mM): 75 NaCl, 2.5 KCl, 25 NaHCO₃, 1.25 NaH₂PO₄, 25 glucose, 0.1 CaCl₂, 6 MgCl₂, and

50 sucrose bubbled with a mixture of 5% CO₂ and 95% O₂, pH 7.4.¹¹ The slices between interaural coordinates 1.50 and 2.10 mm were selected and transferred to artificial cerebrospinal fluid (aCSF) containing (in mM): 125 NaCl, 2.5 KCl, 25 NaHCO₃, 1.25 NaH₂PO₄, 25 glucose, 2 CaCl₂, and 2 MgCl₂, bubbled with a mixture of 5% CO₂ and 95% O₂, pH 7.4, and left to stabilize at room temperature for 30 min.¹¹ After this time, the slices were incubated at 37°C and added with the corresponding reagents in each experiment.

To determine the role of AVP in the upregulated expression of GluA1 and PSD95, as observed in vivo, we evaluated the in vitro effects of exogenous arginine vasopressin AVP applied to the slices in the incubation medium. Six rats were used in this experiment. To obtain sufficient amount of tissue for each blot, tissue from two rats was pooled: one hemisphere for control and one for AVP 100 nM incubation. To determine the time course of exogenous AVP (100 nM) application in the changes observed in the previous experiment, we assayed PSD95 and GluA1 expression under exogenous AVP application (aCSF alone, or aCSF with 100 nM AVP at four time-points: baseline, 5 min, 60 min or 120 min). We used eight rats for this experiment. Brain slices containing ventral hippocampus from the 16 hemispheres were distributed among four time-points and slices from two rats were pooled to run in the same blot. To determine whether the effects were mediated by V1a and/or V1b receptors, we incubated slices from an additional eight (16 hemispheres) during 60 min in aCSF alone, AVP 100 nM, AVP 100 nM plus 100 nM SR49059 or AVP 100 nM plus 100 nM SSR149415. After the incubation, tissue was processed for western blotting through SDS-PAGE electrophoresis as described above.

2.7 | Immunostaining and ExM

Control and WD 48 h male rats ($n = 5$ and $N = 10$) were killed as described and perfused transaortically with 0.9% saline followed by cold fixative containing 4% of paraformaldehyde in 0.1 M phosphate-buffered saline (PBS) (pH 7.4) plus 15% v/v saturated picric acid for 15 min. The brains were sectioned using a VT 1000S vibratome (Leica) at 60 μ m thickness in the horizontal plane.

Sections containing LC were blocked with normal donkey serum (NDS) (20%) in Tris buffered-saline (TBS) (pH 7.4) plus 0.3% Triton-X (TBST) for 1 h and then incubated with the primary antibodies: sheep anti-TH, rabbit anti-AVP, mouse anti-PSD95 and guinea pig anti-GluA1 diluted in TBST plus 1% NDS over two nights, followed by incubation with the corresponding secondary fluorochrome-conjugated antibodies and mounted on glass slides with fluorescent mounting medium and coverslipped. For GluA1 antigen retrieval, slices were first treated with pepsin, 1 mg mL⁻¹ diluted in 0.2 M HCl, and incubated for 10 min at room temperature²³

After conventional imaging, the selected slices were unmounted and processed through a modified ExM technique based on previous protocols.¹⁵⁻¹⁷ Briefly, after washing the slices with PBS (3 \times 15 min at 4°C), slices were anchored with Acryloyl-X (dilution 1:100) in NaHCO₃ (150 mM) buffer overnight at room temperature. Sections

were then washed with PBS and embedded in gelling solution (monomer solution,^{15–17} 4-hydroxy-[2,2,6,6-tetramethylpiperidin-1-yl]oxidanyl, tetramethylethylenediamine, and ammonium persulfate in proportion 47:1:1:1) for 30 min at 4°C. Sections were then immersed in gelling solution in a microscope slide with parafilm, covered with a coverslip and incubated at 37 °C for 2 h. Gel-embedded sections were trimmed to remove excess of gel and digested using 50 mM Tris buffer plus 0.8 M guanidinium chloride, 8 U mL⁻¹ proteinase K, 0.5% Triton X-100, pH 8.0, for 3 h at room temperature. Samples were then washed with PBS (0.28 M, 1 tablet of P4417 [Sigma] in 200 mL of distilled water); no expansion was observed at this time point. When distilled water was used for subsequent washes (three washes, 20 min each), the sample expanded up to 6 times. This ratio of expansion is not adequate for our experimental aims because the target region and signals are largely dispersed, making imaging process difficult. Thus, a modified solution of PBS 0.14 M (half of the concentration of the conventional PBS) was used, obtaining an expansion of approximately 3 times, which made possible the numerical counting of the PSD95 and GluA1 immunopositive puncta at the same time as preserving the neural structure. The samples were flattened in a coverslip treated with poly-L-lysine, with the face of the gel to be imaged toward the coverslip, then mounted in a constructed chamber filled with aqueous mounting medium with the same osmolarity to avoid shrinking.

2.8 | Imaging and quantification of PSD95 and GluA1

Samples were examined in an inverted confocal microscope (LSM 880; Zeiss, Jena, Germany). Images were taken with an optical section of 1 Airy unit (AU). To determine the expansion factor, nuclei of TH positive cells were taken as a reference and diameters were measured in five cells from pre-expanded and five cells from post-expanded samples.

For quantification of PSD95 and GluA1 immunopositive puncta, confocal images taken with a 63× objective on expanded samples were assessed by three investigators who were blind to experimental conditions. Counting was made within an area of 100 μm² (expanded area) and data were analysed for normality and differences obtained with unpaired *t*-test.

2.9 | Statistical analysis

Quantitative results were expressed as the mean ± SEM. The Shapiro–Wilk test was used to confirm their normal distribution. To evaluate differences between means we used Student's *t* test or one-way analysis of variance (ANOVA) followed by Tukey's post-hoc test. All the analyses were performed using Prism, version (GraphPad Software Inc., San Diego, CA, USA). *p* < 0.05 was considered statistically significant. Raw data and results from all the statistical test performed are provided in the Supporting information (Appendix S1).

3 | RESULTS

3.1 | WD increased PSD95 and GluA1 protein expression in amygdala, lateral habenula, and hippocampus

WD for 48 h has previously been shown to activate the AVPMNN system.¹¹ Western blot analysis revealed that 48 h of WD produced a significant increase in amount of protein expression of GluA1 and PSD95 in amygdala, lateral habenula, and ventral hippocampus, comprising three regions that had previously been demonstrated to receive direct innervation from the hypothalamic AVPMNN system.^{9–11,24} In amygdala, three unit-subjects blots were displayed as A1–A3. The consistent increased protein levels of PSD95 and GluA1 were observed after 48 h of WD (Figure 2A1–A3). Bar graphs (Figure 2A4 and A5) show the quantification of the relative protein expression levels compared to control. One-way ANOVA showed that treatment significantly affected the expression of GluA1 ($F_{3,20} = 10.09$, $p < 0.001$) and PSD95 ($F_{3,20} = 17.70$, $p < 0.001$). Tukey multiple comparison test showed significantly higher levels of GluA1 after 48 h WD (1.60 ± 0.129) compared to control (1.00 ± 0.025), 24 h WD (0.983 ± 0.079), and 48 h WD + 24 R (0.716 ± 0.177). PSD95 expression was also increased after 48 h WD (2.067 ± 0.253) compared to control (1.00 ± 0.025), 24 h WD (0.8 ± 0.152) or 48 h + R (0.617 ± 0.083). Likewise, in lateral habenula (Figure 2B), WD treatment significantly affected the expression of GluA1 ($F_{3,20} = 3.479$, $p < 0.05$) and PSD95 ($F_{3,20} = 9.050$, $p < 0.001$). Tukey's multiple comparison test showed increased levels of GluA1 expression after 48 h WD (1.739 ± 0.250) compared to control (1.00 ± 0.079); PSD95 expression was increased after 48 h WD (2.901 ± 0.524) compared to control (1.00 ± 0.033), 24 h WD (1.167 ± 0.244) or 48 h + R (1.104 ± 0.170). In ventral hippocampus, (Figure 2C), correspondingly, 48 h WD treatment significantly affected the expression of GluA1 ($F_{3,20} = 4.154$, $p < 0.05$) and PSD95 ($F_{3,20} = 10.76$, $p < 0.001$). Tukey's multiple comparison test showed significantly higher levels of GluA1 expression after 48 h WD (2.188 ± 0.3) compared to control (1.00 ± 0.201); PSD95 expression was also increased after 48 h WD (2.8 ± 0.549) compared to control (1.00 ± 0.044); 24 h WD (1.033 ± 0.071) or 48 h + R (0.833 ± 0.098). By contrast, in the visual cortex (Figure 2D), where AVPMNN vasopressin direct innervation has not been observed, no significant differences in either PSD95 or GluA1 expression were observed (for a detailed statistical table and descriptive results, see the Supporting information, Appendix S1). In all three regions investigated, a restoration of the expression of GluA1 and PSD95 to control levels was noted after 24 h of recovery from WD.

To show both the individual variability, the consistency among the three unit-subjects, and the reproducibility of the conclusions drawn from the experimental observations, as well as their statistical differences, we chose to show the original western blotting sets of all three unit-subjects in this report.

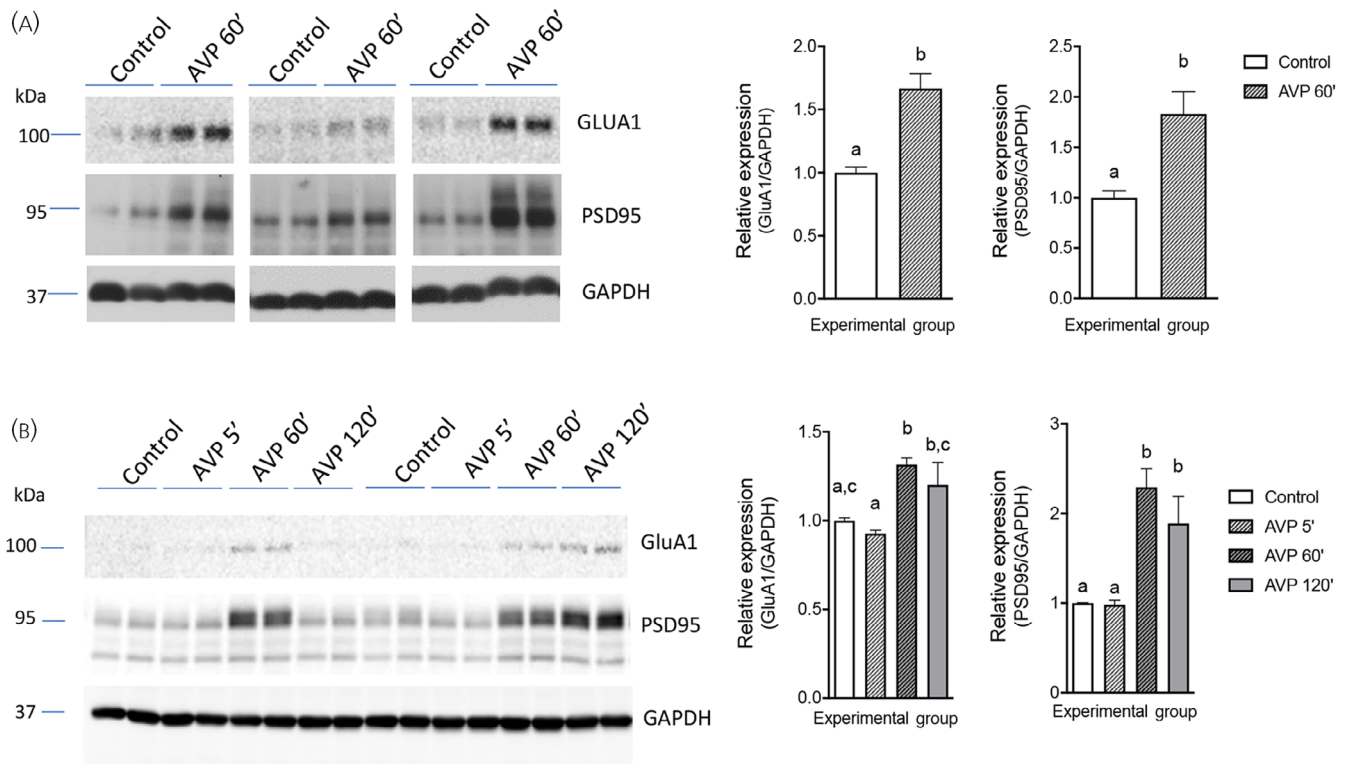


FIGURE 3 Arginine vasopressin (AVP) increased the expression of GluA1 and PSD95 ex vivo. (A) GluA1 (upper blot), PSD95 (middle blot) and GAPDH (lower blot) from lysates of ventral hippocampus formation dissected from acute brain slices (thick 300 μ m) obtained from six rats (two rat samples per each condition), were incubated for 2 h in oxygenated artificial cerebrospinal fluid (aCSF) with vasopressin 100 nM. (B) The relative expression of GluA1 and PSD95 at four time points (tissue from two rats in each lane). Common letter(s) indicate no significant differences between means

3.2 | PSD95 and GluA1 protein expression in vHi slices were increased after incubation with AVP

To assess whether the AVPMNN vasopressinergic innervation to the brain limbic regions assessed above played a prominent role in upregulating the GluA1 and PSD95 expression levels after WD, we performed an ex vivo pharmacological experiment in acute ventral hippocampal slices incubated during 1 h in oxygenated aCSF solution with 100 nM vasopressin.

We selected the ventral hippocampus because of the high level of AVP immunopositive fibres reported in a previous study in which the AVPMNN system was identified as one of the sources of their fibres.⁹ Each blot was constructed from the tissue provided by two rats (one hemisphere for each condition). After 1 h of incubation with 100 nM AVP, we carried out western blotting analysis of the expression of GluA1 or PSD95 protein levels. A two-tailed Student's *t*-test showed that AVP treated slices increased their expression of GluA1 (control: 1.00 ± 0.045 vs. AVP: 1.67 ± 0.117 , $p < 0.01$) and PSD95 (control: 1.00 ± 0.068 vs. AVP: 1.83 ± 0.219 , $p < 0.05$). Three blots and quantification of the relative protein expressions with respect to control are depicted in Figure 3A.

To assess the time course of the AVP effects on postsynaptic proteins expression, we compared ventral hippocampus slices incubated in oxygenated aCSF (control) or exposed to 5, 60 or 120 min of aCSF

with addition of 100 nM AVP. A total of eight rats provided the tissue for this experiment (four hemispheres per condition). Two-way ANOVA showed an effect of treatment for GluA1 ($F_{3,28} = 7.049$, $p < 0.01$) and for PSD95 ($F_{3,28} = 17.5$, $p < 0.001$). Post-hoc Tukey multiple comparison test showed a significant increase of GluA1 at 60 minutes of AVP exposure (1.315 ± 0.037) compared to control (1 ± 0.015). For PSD95, significantly higher expression levels were found after 60 min (2.29 ± 0.179) and 120 min of AVP exposure (1.89 ± 0.251) compared to control (1 ± 0.024). Quantification of the relative protein expressions for each time point with respect to control is depicted in Figure 3B.

3.3 | Vasopressin induced increase of GluA1 and PSD95 expression in vHi slices is blocked after incubation with AVP receptor antagonists

Because both V1a and V1b vasopressin receptors have been reported to be present in the hippocampus.^{25,26} We investigated whether antagonists for either receptor could revert the AVP-induced increase in GluA1 and PSD95 expression. Eight rats were used to obtain ventral hippocampus slices for incubation in aCSF (control), AVP 100 nM, AVP 100 nM + SR49059 100 nM, or AVP 100 nM + SSR149415 100 nM. Following a 60-min incubation period, GluA1 and PSD95 levels

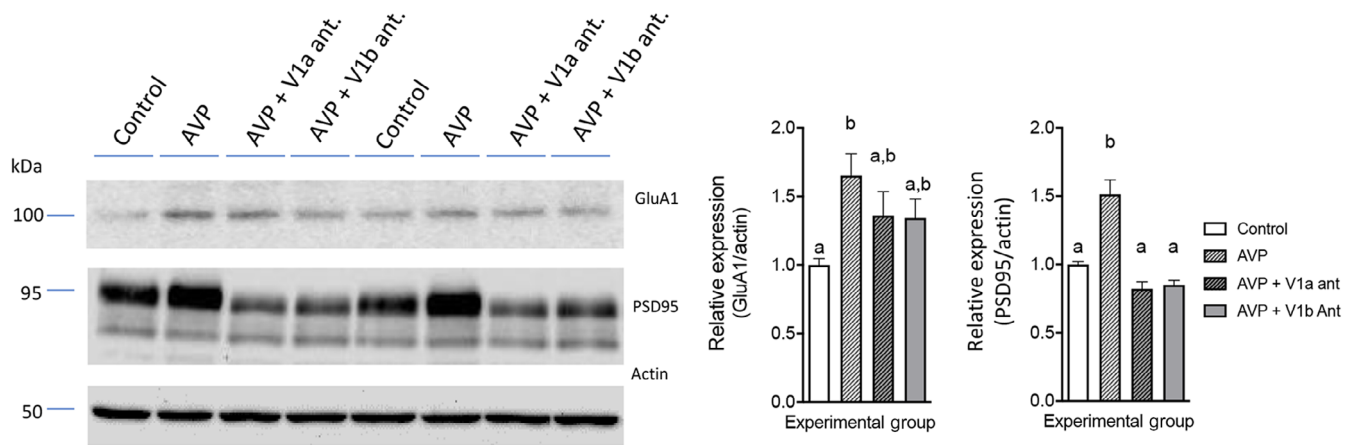


FIGURE 4 Arginine vasopressin (AVP) induced increase in the expression of GluA1 and PSD95 ex vivo was blocked by V1a and V1b receptor antagonists. Left: GluA1 (upper blot), PSD95 (middle blot) and actin (lower blot) from lysates of ventral hippocampus formation, dissected from acute brain slices obtained from eight rats (16 hemispheres), which were incubated for 1 h in oxygenated artificial cerebrospinal fluid (aCSF) with vasopressin 100 nM (AVP), AVP plus the V1a receptor selective antagonist (SR49059) or AVP plus the selective V1b receptor antagonist (SSR149415). Left bar graph: Relative expression (mean ± SEM) of GluA1. Right bar graph: Relative expression (mean ± SEM) of PSD95. Bars that do not share a letter indicate significant differences between means

were assessed by western blotting and their relative expression (normalised to control) was compared by a two-way ANOVA. Significant effect of treatment was observed for GluA1 ($F_{3,28} = 3.664$, $p < 0.05$) and PSD95 ($F_{3,28} = 28.19$, $p < 0.001$). Tukey's multiple comparisons test showed that, compared to control, AVP treated slices had significantly increased expression of GluA1 (AVP: 1.652 ± 0.455 vs. control: 1 ± 0.132) and PSD95 (AVP: 1.514 ± 0.046 vs. control: 1 ± 0.161). Slices incubated with AVP and equimolar concentrations of V1a antagonist (SR49059) or V1b antagonist (SSR149415) blocked the effects of AVP, although the effect on GluA1 was less prominent than that on PSD95 (Figure 4).

3.4 | WD increased the PSD95 and GluA1 immunopositive puncta's densities in TH+ dendritic compartment in the LC: puncta in apposition to AVP+ axonal varicosities

After observing the augmentation in the amounts of PSD95 and GluA1 following WD in vivo and AVP ex vivo exposure, with western blotting, we aimed to evaluate whether WD increases the PSD95 and GluA1 immunopositive puncta densities in a given brain region innervated by AVPMNN direct projections. We chose the pontine LC as an example of a region densely innervated by AVP-immunopositive fibres that increases with WD (Figure 5A,B).¹² The rationale of this selection is that the strong somatic/dendritic expression of TH of the noradrenergic neurons in LC and its cellular homogeneity would help us to overcome the difficulties caused by immunofluorescence signal decay during the ExM processing. It is worth noting that the optical resolution of conventional immunofluorescence confocal microscopy limits the clear quantification of postsynaptic density proteins. Figure 5C shows a TH immunopositive neuron (diameter of nucleus: 7 μ m) and

its inset shows the triple immunofluorescence reaction, before ExM processing, where the signals from TH, AVP, and GluA1 (blue, red, and green, respectively) are (partially, at least) overlapping, indicated with pink arrows. With the modified expansion microscopy (2–3 times), this quantification is achievable, at the same time as conserving the regional/cellular structure and easy handling for microscopical examination. Figure 5D shows an expanded TH+ positive neuron (diameter of nucleus: 21 μ m) with well conserved somatodendritic cytoarchitecture. Inset, taking from the same sample, shows clear separation of the three immunofluorescence signals (TH, AVP, and GluA1 [blue, red, and green, respectively]) indicated by corresponding arrows). Appositions between AVP axons (red), TH+ dendrites containing GluA1/PSD95 puncta (green) are depicted in Figure 5E–G. Figure 5E and E' are photomicrographs of TH/AVP/GluA1 or TH/AVP/PSD95, respectively, from control rats. Figure 5F1–F4 and Figure 5G1–G4 are taken from the same regions of Figure 5F and Figure 5G for rats that underwent 48 h of WD, with further digitally magnification, in different Z levels, showing the abundance of these two PSD proteins in dendritic compartments. AVP axonal varicosity in apposition to TH+ dendrite, containing PSD proteins is indicated with asterisks. This latter aspect is exemplified at ultrastructural level with Figure 5H, which is a representative electron micrograph taken from reference,¹² showing an AVP-containing axon terminal establishing a Gray type I synapse on the TH+ dendrite. A comparison of GluA1 and PSD95 puncta's density in the LC TH+ dendritic compartments was performed on expanded immunoreacted slices from rats ($n = 5$, $N = 10$) that underwent 48 h of WD (WD 48 h) against those that were under food and water ad libitum conditions. A Student's *t* test showed that WD 48 h produced a significant increase in the density of GluA1 (WD 48 h: 10.7 ± 0.633 vs. 6.8 ± 0.633 , $p < 0.001$) and PSD95 (WD 48 h: 16.5 ± 0.992 vs. 9.9 ± 1.22 , $p < 0.001$) puncta per 100 μ m² of TH+ dendritic compartments on the expanded confocal

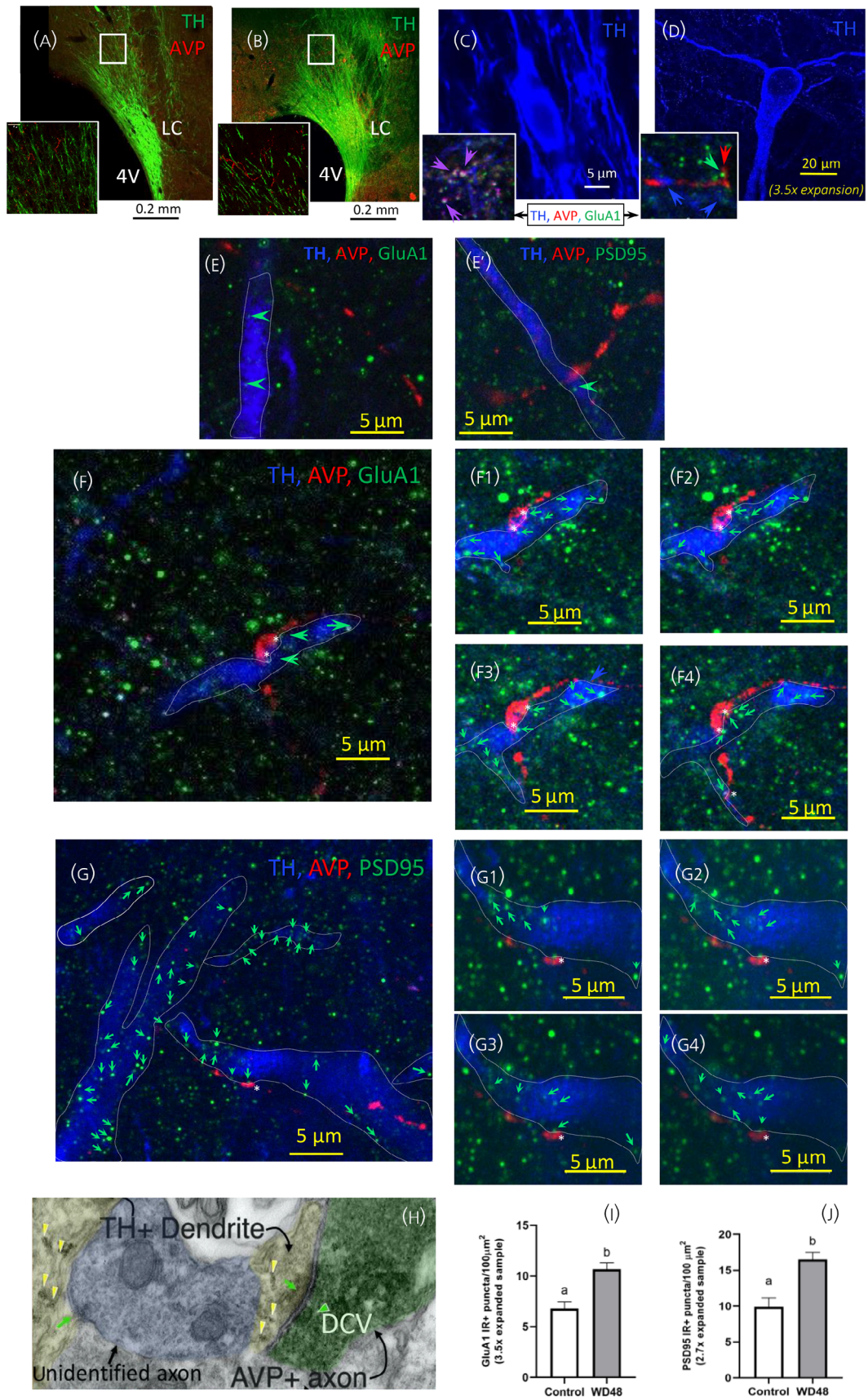


FIGURE 5 Legend on next page.

(1 Airy unit = 0.68 μm optical section thickness) photomicrograph. The results of the comparison are shown as the mean \pm SEM in the bar graph of Figure 5I,J.

4 | DISCUSSION

In the present study, we investigated the dynamic changes of PSD95 and GluA1 expression levels and their localization in response to WD and AVP. Our data unambiguously demonstrated the augmentation of these PSD proteins amounts in 48 h WD animals, in brain limbic regions receiving direct ascending projections from AVPMNN. By contrast, in the visual cortex, a region in which AVPMNN innervation has not been observed, this phenomenon did not occur. The neuropeptide vasopressin's involvement in this phenomenon is further demonstrated through pharmacological exposure of AVP (100 nm), directly to brain ventral hippocampal slices *ex vivo*, with the strongest effect observed after 60 min of exposure, using western blotting. We interpret the difference in the prompt effects of AVP *ex vivo*, compared to the delayed effects of WD, to reflect the time required for WD to trigger consequential increases in AVP release *in vivo*. The inhibition of AVP stimulation of GluA1 and PSD95 expression was expected to be via V1a and/or V1b receptors in the ventral hippocampus. Either the V1a or the V1b antagonist ablated the AVP-stimulated increases on PSD95 or GLUA1 expression as measured by western blotting (conclusion based on the absence of statistically significant differences observed compared to control). This suggests that a cooperative activation of V1a and V1b receptors is needed for the AVP-induced postsynaptic protein potentiation. However, it will require an extensive set of experiments to confirm it, which is beyond the scope of the present study. However, the failure to provide a detailed explanation does not detract from the main demonstration that antagonists ablated the AVP stimulated increase in postsynaptic protein expression.

We detected, quantitatively, an enrichment of PSD proteins' immunopositive puncta on LC principal neuron dendrites, and also observed the close appositions between AVP axon terminals and both

GluA1 and PSD95 puncta within TH immunopositive dendrites, which indicates the existence of excitatory synapses established by presynaptic vasopressin-containing axons. These data were obtained using the newly developed expansion microscopy method, modifying the published protocols to a lower expansion ratio that is sufficient for the purpose of the present study, at the same time as facilitating handling for microscopical examination.

The synapse is a highly complex subcellular specialization involving closely apposed pre- and postsynaptic membranes and a prominent molecular machinery associated with them that enables chemical-electrical transmission between neurons, and its dynamic adaptation in response to experience.²⁷ In excitatory post-synapses, a set of molecules is assembled in an ultrastructural feature known as the PSD, a narrow electron-dense area subjacent to the postsynaptic membrane.^{8,28} The PSD is composed of several scaffolding proteins that coordinate the trafficking and membrane insertion of AMPA- or NMDA-type glutamate ionotropic receptors at the synaptic cleft, thus allowing excitatory transmitter-dependent activation of the postsynaptic neuron and stabilizing synaptic contact.²⁹⁻³⁵ This dynamic process appears to be finely tuned by various cues that include autocrine, paracrine, and neurocrine signals occurring at the synaptic cleft or in the vicinity of the synapse, which can modulate molecular pathways within the PSD, allowing short- and long-term regulation of synaptic plasticity.^{36,37} We chose to investigate the neurohormone vasopressin's effect(s) on the above physiological process, through determination of changes in the expression of the glutamate AMPAR receptor subunit GluA1, a molecule that has been reported to be mainly localized within glutamatergic synapses and is hence an excitatory synapse marker,³⁸ and PSD95, a membrane-associated guanylate kinase. Both PSD95 and GluA1 are crucial regulators of postsynaptic organization and function.^{39,40} We focused on limbic projections domains of AVPMNN,^{9-11,24,41} in comparison with non-AVP-innervated brain areas, and under conditions in which the AVPMNN system is dramatically upregulated.^{20,42} We have shown that WD causes prompt enhancement of PSD95 and GluA1 levels in limbic brain areas to

FIGURE 5 Water deprivation increased the density of GluA1 and PSD95 immunopositive puncta in the tyrosine hydroxylase (TH) immunopositive dendritic compartment in the locus coeruleus (LC). (A, B) Representative LC photomicrographs in control and 48 h of water deprivation (48 h WD) rats. WD48 increased arginine vasopressin (AVP) immunoreactivity (red) located in the region where dendrites immunopositive for TH (green) are abundant. 4V, fourth ventricle. (C, D) Confocal photomicrographs (63 \times objective used in both case) of TH immunopositive neurons before (C) and after (D) expansion microscopy (ExM). An increase of approximately 3 times the soma size (note that the diameters of the nucleus increased from 7 μm to 21 μm) was observed after expansion (white or yellow scale bars indicate pre-ExM and post-ExM photomicrographs, respectively). In the high magnification confocal (1 Airy unit) images depicted in the insets, that before ExM (C), the GluA1 puncta are confluent (pink arrows) and, after ExM (D), the GluA1 puncta (green) are separated from other two-colored signals (red, green, and blue arrows indicate AVP, GluA1 and TH immunopositive compartments, respectively). Note that the background noise is also lowered by ExM processing. (E) to (G) Examples of post-ExM photomicrographs of GluA1 (Es) or PSD95 (Fs) immunoreacted sections respectively. (E) (E') Photomicrographs of TH/AVP/GluA1 or TH/AVP/PSD95, respectively, from control rats. Subpanels (F1-F4 and G1-G4) are taken from the same regions of (F) and (G), with further digital magnification, in different Z levels, showing the abundance of these two postsynaptic density (PSD) proteins in TH+ dendritic compartments. AVP axonal varicosity in apposition to TH+ dendrite, containing PSD proteins are indicated with white asterisks. (H) Electron photomicrograph shows ultrastructural evidence of the existence of putative glutamatergic (asymmetric) synapses between AVP+ axon and TH immunopositive dendritic segment within the LC. Green arrowheads show dense core vesicles (DCV) typical of peptidergic transmission (taken from Hernandez-Perez et al.¹²; creative Commons Attribution License holder). (I) to (J) Bar graphs show the mean \pm SEMs of the GluA1 and PSD95 puncta density in control and WD48 rats, respectively. Quantification was made after ExM within TH+ dendritic compartment in the LC. Different letters above the bars indicate significant differences between groups. Scale bars for expanded samples are yellow

which AVP-glutamatergic neurons project, although not in primary visual cortex, an area in which expression of these proteins is equally abundant, but which do not receive AVPMNN innervation. Augmentation of PSD95 and GluA1 was reversible upon re-institution of water availability, indicating the state-dependency of this effect. These data reveal a novel role for AVP as a synapse organizer in limbic regions innervated by AVPMNN direct projections, a potential mechanistic link between homeostatic adversity (WD) and motivational drive.

We have previously shown that water-deprived animals exposed to cat odour show diminished freezing behaviour and reduced functional output of lateral habenula, likely as a result of selective activation of GABAergic interneurons in this region selectively receiving glutamate-vasopressin innervation,^{11,43} suggesting that the vasopressinergic system could act as a modulator of synaptic transmission during stress responses. The present data add concrete cellular data about the possible mechanisms by which vasopressin alters synaptic function under conditions of stress (in this case, WD) by regulation of two discrete postsynaptic density proteins, PSD95 and GluA1, and extends it to other brain regions innervated by AVPMNNs, including the amygdala and ventral hippocampus. This modulation could well be of physiological importance with respect to influencing decision-making leading to behavioural responses that facilitate survival in the face of homeostatic and environmental threats.

Technical considerations

Although the *in vivo* employment of antagonists to demonstrate specificity would be desirable, via microinjection or systematic administration, for the particular aim of the present study (i.e., postsynaptic density protein expression level changes in specific brain regions), they have major limitations because systemic or microinjection delivery cannot adequately neutralize the *in vivo* delivery of AVP directly into the synapse. This might be overcome by utilizing mice with ablation of V1a and V1b receptor genes. However, this would have to be conditional knock-out because the animals might not be viable or have undergone physiological buffering (re-organization) if ablation is ab initio.

We continue to search for experiments to further demonstrate the mechanism of AVP-induced synaptic protein regulation. Performing similar experiments in mouse will allow genetic ablation of V1a and V1b to confirm, *in vivo*, the importance of each receptor subtype for PSD95 and GluA1 regulation by WD. Although this is beyond the scope of the present work, we consider it a necessary extension of the results reported here *ex vivo* (in slice preparation), and will pave the way for understanding how each receptor type signals to effect this dramatic modulation

AUTHOR CONTRIBUTIONS

Limei Zhang: Conceptualization; data curation; formal analysis; funding acquisition; investigation; methodology; resources; supervision; validation; visualization; writing – original draft; writing – review and editing. **Teresa Padilla-Flores:** Data curation; formal analysis; investigation; methodology. **Vito Salvador Hernandez:** Conceptualization; data curation; formal analysis; investigation; methodology; project administration; resources; software; supervision; validation; visualization; writing – original draft; writing – review and editing. **Mario Alberto Zetter:** Data curation; formal analysis; supervision; validation; visualization; writing – original draft; writing –

review and editing. **Elba Campos-Lira:** Data curation; investigation; methodology; writing – review and editing. **Laura I. Escobar:** Resources; supervision; writing – review and editing. **Robert P Millar:** Formal analysis; methodology; supervision; writing – review and editing. **Lee E Eiden:** Conceptualization; funding acquisition; resources; supervision; validation; writing – original draft; writing – review and editing.

ACKNOWLEDGMENTS

We thank Maurice Manning for his kind gift of arginine vasopressin, as well as María del Carmen Cardenas-Aguayo for helping with the western blotting experiments. MAZ is grateful for a UNAM-DGAPA-POSDOC fellowship. TPF and ECL are grateful for the support of a CONACYT PhD studentship through grant CONACYT-CB-238744. RPM wishes to thank the UNAM-DGAPA-PREI program for the support of his sabbatical stay at the LZ lab. LZ wishes to express her gratitude to Peter Somogyi for hosting her second sabbatical year (2007–2008), during which an in depth discussion on her electron microscopy observations spawned the present study. This project was supported by grants: UNAM-DGAPA-PAPIIT-IN200121 & CONACYT-CB-238744 and 283279 (LZ); CONACYT A1-S-8731 (LIE); NIMH-IRP, NIH, ZIAMH0002386 (LEE).

DATA AVAILABILITY STATEMENT

The data that support the findings of this study are available on request from the corresponding author. The data are not publicly available due to privacy or ethical restrictions.

ORCID

Limei Zhang  <https://orcid.org/0000-0002-7422-5136>

Vito S. Hernández  <https://orcid.org/0000-0002-1486-1659>

Mario A. Zetter  <https://orcid.org/0000-0001-7132-5345>

Laura I. Escobar  <https://orcid.org/0000-0002-5142-8993>

Robert P. Millar  <https://orcid.org/0000-0003-3606-2708>

Lee E. Eiden  <https://orcid.org/0000-0001-7524-944X>

REFERENCES

- Boone M, Deen PM. Physiology and pathophysiology of the vasopressin-regulated renal water reabsorption. *Pflugers Arch*. 2008; 456(6):1005-1024.
- Bargmann W, Scharrer E. The site of origin of the hormones of the posterior pituitary. *Am Sci*. 1951;39(2):255-259.
- Pow DV, Morris JF. Dendrites of hypothalamic magnocellular neurons release neurohypophysial peptides by exocytosis. *Neuroscience*. 1989; 32(2):435-439.
- Brown CH, Ludwig M, Tasker JG, Stern JE. Somato-dendritic vasopressin and oxytocin secretion in endocrine and autonomic regulation. *J Neuroendocrinol*. 2020;32(6):e12856.
- De Wied D. Long term effect of vasopressin on the maintenance of a conditioned avoidance response in rats. *Nature*. 1971;232(5305):58-60.
- de Wied D. Behavioral effects of intraventricularly administered vasopressin and vasopressin fragments. *Life Sci*. 1976;19(5):685-690.
- Muhlethaler M, Dreifuss JJ, Gahwiler BH. Vasopressin excites hippocampal neurones. *Nature*. 1982;296(5859):749-751.
- Peters A. *The Fine Structure of the Nervous System*. Harper Row; 1970.
- Zhang L, Hernandez VS. Synaptic innervation to rat hippocampus by vasopressin-immuno-positive fibres from the hypothalamic supraoptic and paraventricular nuclei. *Neuroscience*. 2013;228:139-162.

10. Hernandez VS, Hernandez OR, Perez de la Mora M, et al. Hypothalamic Vasopressinergic projections innervate central amygdala GABAergic neurons: implications for anxiety and stress coping. *Front Neural Circuits*. 2016;10:92.
11. Zhang L, Hernandez VS, Vazquez-Juarez E, Chay FK, Barrio RA. Thirst is associated with suppression of Habenula output and active stress coping: is there a role for a non-canonical vasopressin-glutamate pathway? *Front Neural Circuits*. 2016;10:13.
12. Hernandez-Perez OR, Hernandez VS, Nava-Kopp AT, et al. A Synaptically connected hypothalamic magnocellular vasopressin-locus Coeruleus neuronal circuit and its plasticity in response to emotional and physiological stress. *Front Neurosci*. 2019;13:196.
13. Zhang L, Hernández VS, Murphy D, Young WS, Eiden LE. Fine chemo-anatomy of hypothalamic magnocellular Vasopressinergic system with an emphasis on ascending connections for Behavioural adaptation. In: Valery Grinevich AD, ed. *Neuroanatomy of Neuroendocrine Systems*. Springer; 2022:167-196.
14. Zhang L, Eiden LE. Two ancient neuropeptides, PACAP and AVP, modulate motivated behavior at synapses in the extrahypothalamic brain: a study in contrast. *Cell Tissue Res*. 2019;375(1):103-122.
15. Tillberg PW, Chen F, Piatkevich KD, et al. Protein-retention expansion microscopy of cells and tissues labeled using standard fluorescent proteins and antibodies. *Nat Biotechnol*. 2016;34(9):987-992.
16. Asano SM, Gao R, Wassie AT, Tillberg PW, Chen F, Boyden ES. Expansion microscopy: protocols for imaging proteins and RNA in cells and tissues. *Curr Protoc Cell Biol*. 2018;80(1):e56.
17. Truckenbrodt S, Sommer C, Rizzoli SO, Danzl JG. A practical guide to optimization in X10 expansion microscopy. *Nat Protoc*. 2019;14(3):832-863.
18. Manning M, Misicka A, Olma A, et al. Oxytocin and vasopressin agonists and antagonists as research tools and potential therapeutics. *J Neuroendocrinol*. 2012;24(4):609-628.
19. Buijs R, Pool C, Van Heerikhuizen J, et al. Antibodies to small transmitter molecules and peptides: production and application of antibodies to dopamine, serotonin, GABA, vasopressin, vasoactive intestinal peptide, neuropeptide Y, somatostatin and substance P. *Biomed Res*. 1989;10(supplement 3):213-221.
20. Dunn FL, Brennan TJ, Nelson AE, Robertson GL. The role of blood osmolality and volume in regulating vasopressin secretion in the rat. *J Clin Invest*. 1973;52(12):3212-3219.
21. Chafai M, Corbani M, Guillon G, Desarmenien MG. Vasopressin inhibits LTP in the CA2 mouse hippocampal area. *PLoS One*. 2012;7(12):e49708.
22. Mruk DD, Cheng CY. Enhanced chemiluminescence (ECL) for routine immunoblotting: an inexpensive alternative to commercially available kits. *Spermatogenesis*. 2011;1(2):121-122.
23. Polgar E, Watanabe M, Hartmann B, Grant SG, Todd AJ. Expression of AMPA receptor subunits at synapses in laminae I-III of the rodent spinal dorsal horn. *Mol Pain*. 2008;45:1744-8069-4-5.
24. Cui Z, Gerfen CR, Young WS 3rd. Hypothalamic and other connections with dorsal CA2 area of the mouse hippocampus. *J Comp Neurol*. 2013;521(8):1844-1866.
25. Ostrowski NL, Lolait SJ, Young WS 3rd. Cellular localization of vasopressin V1a receptor messenger ribonucleic acid in adult male rat brain, pineal, and brain vasculature. *Endocrinology*. 1994;135(4):1511-1528.
26. Vaccari C, Lolait SJ, Ostrowski NL. Comparative distribution of vasopressin V1b and oxytocin receptor messenger ribonucleic acids in brain. *Endocrinology*. 1998;139(12):5015-5033.
27. Somogyi P, Tamas G, Lujan R, Buhl EH. Salient features of synaptic organization in the cerebral cortex. *Brain Res Brain Res Rev*. 1998;26(2-3):113-135.
28. Boeckers TM. The postsynaptic density. *Cell Tissue Res*. 2006;326(2):409-422.
29. Ehrlich I, Klein M, Rumpel S, Malinow R. PSD-95 is required for activity-driven synapse stabilization. *Proc Natl Acad Sci U S A*. 2007;104(10):4176-4181.
30. Coley AA, Gao WJ. PSD-95 deficiency disrupts PFC-associated function and behavior during neurodevelopment. *Sci Rep*. 2019;9(1):9486.
31. Kim MJ, Futai K, Jo J, Hayashi Y, Cho K, Sheng M. Synaptic accumulation of PSD-95 and synaptic function regulated by phosphorylation of serine-295 of PSD-95. *Neuron*. 2007;56(3):488-502.
32. Kennedy MB. Signal-processing machines at the postsynaptic density. *Science*. 2000;290(5492):750-754.
33. Ehrlich I, Malinow R. Postsynaptic density 95 controls AMPA receptor incorporation during long-term potentiation and experience-driven synaptic plasticity. *J Neurosci*. 2004;24(4):916-927.
34. Taft CE, Turrigiano GG. PSD-95 promotes the stabilization of young synaptic contacts. *Philos Trans R Soc Lond B Biol Sci*. 2014;369(1633):20130134.
35. Uchino S, Wada H, Honda S, et al. Direct interaction of post-synaptic density-95/Dlg/ZO-1 domain-containing synaptic molecule Shank3 with GluR1 alpha-amino-3-hydroxy-5-methyl-4-isoxazole propionic acid receptor. *J Neurochem*. 2006;97(4):1203-1214.
36. Rodrigues SM, Schafe GE, LeDoux JE. Molecular mechanisms underlying emotional learning and memory in the lateral amygdala. *Neuron*. 2004;44(1):75-91.
37. Park H, Rhee J, Park K, Han JS, Malinow R, Chung C. Exposure to stressors facilitates long-term synaptic potentiation in the lateral Habenula. *J Neurosci*. 2017;37(25):6021-6030.
38. Diering GH, Hagan RL. The AMPA receptor code of synaptic plasticity. *Neuron*. 2018;100(2):314-329.
39. Ziff EB. Enlightening the postsynaptic density. *Neuron*. 1997;19(6):1163-1174.
40. Chen X, Levy JM, Hou A, et al. PSD-95 family MAGUKs are essential for anchoring AMPA and NMDA receptor complexes at the postsynaptic density. *Proc Natl Acad Sci U S A*. 2015;112(50):E6983-E6992.
41. Hernandez V, Vazquez-Juarez E, Márquez MM, Jáuregui-Huerta F, Barrio R, Zhang L. Extra-neurohypophyseal axonal projections from individual vasopressin-containing magnocellular neurons in rat hypothalamus. *Frontier in Neuroanatomy*. 2015;9:130.
42. Zhang L, Medina MP, Hernandez VS, Estrada FS, Vega-Gonzalez A. Vasopressinergic network abnormalities potentiate conditioned anxious state of rats subjected to maternal hyperthyroidism. *Neuroscience*. 2010;168(2):416-428.
43. Zhang L, Hernandez VS, Swinny JD, et al. A GABAergic cell type in the lateral habenula links hypothalamic homeostatic and midbrain motivation circuits with sex steroid signaling. *Transl Psychiatry*. 2018;8(1):50.

SUPPORTING INFORMATION

Additional supporting information may be found in the online version of the article at the publisher's website.

How to cite this article: Zhang L, Padilla-Flores T, Hernández VS, et al. Vasopressin acts as a synapse organizer in limbic regions by boosting PSD95 and GluA1 expression. *J Neuroendocrinol*. 2022;34(9):e13164. doi:10.1111/jne.13164